Asymmetric exclusion processes with fixed resources: Reservoir crowding and steady states

Astik Haldar,[1,*] Parna Roy,[2,†] and Abhik Basu[1,‡]
[1]*Theory Division, Saha Institute of Nuclear Physics, HBNI, Calcutta 700064, West Bengal, India*
[2]*Shahid Matangini Hazra Government College for Women, Purba Medinipore 721649, West Bengal, India*

(Received 15 September 2020; accepted 6 August 2021; published 7 September 2021)

We study the reservoir crowding effect by considering the nonequilibrium steady states of an asymmetric exclusion process (TASEP) coupled to a reservoir with fixed available resources and dynamically coupled entry and exit rate. We elucidate how the steady states are controlled by the interplay between the coupled entry and exit rates, both being dynamically controlled by the reservoir population, and the fixed total particle number in the system. The TASEP can be in the low-density, high-density, maximal current, and shock phases. We show that such a TASEP is different from an open TASEP for *all* values of available resources: here the TASEP can support only localized domain walls for any (finite) amount of resources that do not tend to delocalize even for large resources, a feature attributed to the form of the dynamic coupling between the entry and exit rates. Furthermore, in the limit of infinite resources, in contrast to an open TASEP, the TASEP can be found in its high-density phase only for any finite values of the control parameters, again as a consequence of the coupling between the entry and exit rates.

DOI: 10.1103/PhysRevE.104.034106

I. INTRODUCTION

An overall theoretical understanding of nonequilibrium driven diffusive systems, with potential connections with hosts of natural phenomena, remains elusive today. In the absence of any general theoretical framework to study nonequilibrium systems, it is useful to consider and study simple model systems, where explicit calculations can be performed easily, helping to develop wide-ranging physical intuitions. The totally asymmetric simple exclusion process (TASEP), an archetypal driven system, was originally introduced as a conceptual model for describing protein synthesis in biological cells [1]. Later it emerged as a paradigmatic model for boundary-induced nonequilibrium phase transitions in one dimension [2]. Unlike a TASEP with open boundary conditions, TASEPs in closed geometries strictly conserve the total particle number. A TASEP on a ring with a single point defect has been studied in Ref. [3] that shows a localized domain wall (LDW) for intermediate densities. An open TASEP with a global constraint on the total particle number, i.e., a TASEP connected with a particle reservoir of finite capacity or a particle storage [4–8], is distinct from a conventional open TASEP or a TASEP on a ring. These models, broadly called TASEPs with finite resources, are expected to be relevant in related biological processes of protein synthesis in cells [4] and also in the context of traffic [9]; see also Ref. [10] for a similar study. In these models, the primary effect of the finiteness of the available resources is that the effective entry rate of the particles to the TASEP, e.g., the actual protein synthesis taking place, sensitively depends upon the available resources. Detailed studies, both numerical MCS and analytical MFT, reveal rich nonuniform steady-state density profiles including pinning of domain walls in these models [4–8]. These have been applied to various different problems, e.g., limited resources in driven diffusive systems [11], different biological contexts like mRNA translations and motor protein dynamics in cells [12], and traffic problems [9]. Notable experimental studies relevant to these model systems include studies on spindles in eukaryotic cells [13]. From the standpoint of nonequilibrium statistical mechanics, these models serve as minimal models for "nonequilibrium phase transitions with a global conservation law."

In the existing models for TASEPs with finite resources, the exit rates from the TASEP lanes are unaffected by the reservoir population. It is, however, reasonable to expect that a crowded reservoir (i.e., with "high" reservoir occupation) not only facilitates entry of particles into the TASEP but may also hinder particles leaving TASEP as well. This can potentially lead to a very low current in the TASEP in the steady state in the limit of high reservoir occupation. In this work, we explore a simple mechanism for avoidance of a crowded reservoir by the particles or agents, i.e., the particles are *more inclined* to leave the reservoir, but *more inhibited* to return to it, if the latter gets more crowded. We show that this ensures that even in the limit of infinite resources, the TASEP connected to a reservoir remains qualitatively different from a TASEP with open boundary conditions. We call this the "reservoir crowding effect" and model this in terms of "effective entry and exit rates," both of which depend upon the instantaneous reservoir occupation and which are mutually coupled. In this article we study how this can affect the NESS of the TASEP connected to it.

We introduce and systematically study a simple minimal model for reservoir crowding that consists of a single TASEP

*astik.haldar@gmail.com
†parna.roy14@gmail.com
‡abhik.123@gmail.com, abhik.basu@saha.ac.in

lane that is connected to a reservoir without any spatial extent at both its ends and having both its entry and exit rates being controlled dynamically by the reservoir population. The dynamical control of both the actual entry and exit rates by the same quantity (reservoir population) naturally introduces a coupling between the two rates that, to our best knowledge, along with its effects on the steady states are considered here for the first time. This dynamic coupling between the entry and exit rates clearly sets our model apart from the existing models. This model is parametrized by three parameters: α and β that parametrize the actual entry and exit rates of the TASEP lane, and μ, which is a measure of the total particle number (see the next section for more precise definitions of these parameters). Our principal results are as follows. Its NESS admits four distinct phases: low-density (LD), high-density (HD), maximal current (MC), and shock (SP) phases: (i) In general, the phase diagram of this model in the α-β plane is very different from that of an open TASEP as parametrized by the model parameters; by tuning α, β, the TASEP can preferentially be populated or depopulated. More specifically, (ii) the well-known first-order transition between the LD and HD phases in an open TASEP is replaced by *two* second-order transitions, one between the LD and SP phases, and another between the SP and HD phases. The system shows generic LDWs in the SP phase. Unexpectedly and in contrast to the results in Ref. [14], the LDWs remain pinned for *any* particle number or any resources in the system and show no tendency to delocalize even in the limit of very large resources for which the effects of the particle number conservation is naïvely expected to be unimportant. (iii) In the limit of large μ, the phase diagram of the TASEP does not approach that of an open TASEP [7]; instead it can only be in its HD phase. We argue that these results are linked to the dynamical coupling between the entry and the exit rates introduced in this model, and make the present model fundamentally different from the existing models of TASEPs with finite resources, where the exit rates are taken to be fixed [7]. This is one of the aspects of our model that directly brings out the essence of the *reservoir crowding effect*, the main thrust of the present work.

Our model serves as a minimal 1D nonequilibrium model to study the crowding effect, and how it gets affected by the dynamical coupling between the effective entry and exit rates. This should be useful in transport problems where the agents actively prefer to avoid getting stuck in crowded intersections or stations by either exiting from it quicker or entering into it slower, depending upon the degree of crowd. Consider, e.g., a fixed number of vehicles in a closed network of roads with a toll plaza or a drive-in (any place where several vehicles would wait at any given time for some specific purposes, that may serve as a "pool" or "reservoir" of vehicles). In addition, this model can serve as the simplest representation of devices connected to particle sources and sinks having tunable entry and exit rates for the particles that are mutually coupled in some manner by virtue of their dependences on a single quantity, e.g., reservoir population.

The rest of the article is organized as follows. In Sec. II we have introduced and defined the model. In Sec. III we heuristically argue the nature of the steady states. We also present a series of phase diagrams in the $\alpha - \beta$ plane for various values of μ, which highlight the sensitive dependences of the phase boundaries on μ. Next, in Sec. IV mean-field theory (MFT) analysis of our model along with the phase diagrams and the steady-state density profiles, complemented by extensive Monte Carlo simulation (MCS) studies, are presented. Then in Sec. V we discuss the nature of the phase transitions in the models. In Sec. VI we analyze the nature of the domain walls, including their pinning for large resources. We end by summarizing our results in Sec. VII.

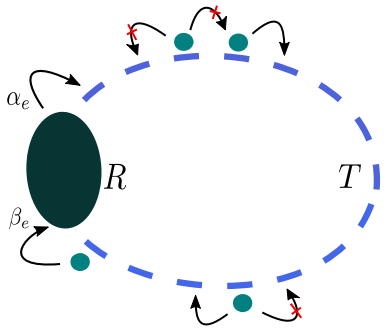

FIG. 1. Schematic model diagram: the filled (deep green) ellipse R is the point reservoir of infinite capacity; the broken line T is the TASEP lane with L sites connected to R at both the ends, with α_e and β_e being the effective entry and exit rates of T. Small (light green) circles represent particles that hop along T, subject to asymmetric exclusion process (see text).

II. MODEL

The model consists of a single TASEP lane T connected at both its ends to a reservoir R. The particles from R enter T through its entry end, hop unidirectionally along T subject to exclusion, and eventually leave T at its exit end and enter back into R; see Fig. 1. Due to the closed geometry of the system, the dynamics clearly conserves the total particle number N_0. The reservoir R is a point reservoir, without any spatial extent or internal dynamics, and can accommodate any number of particles without any upper limit.

TASEP lane T has L sites, which are labeled by i; $i \in [1, L]$ with $i = 1$ and $i = L$ being at the entry and exit sides, respectively. The entry and exit rates of T are parametrized by α and β, respectively, which can take any positive values without restrictions. The actual entry and exit rates are dynamically controlled and are given by

$$\alpha_e = \alpha f(N), \;\; \beta_e = \beta g(N), \tag{1}$$

where N is the instantaneous occupation of R. We define filling factor $\mu = N_0/L$, which describes the population of the whole model (T and R combined) relative to the size L of T; thus $0 \leqslant \mu \leqslant \infty$. Our model, therefore, is a three-parameter model: the NESS are parametrized by α, β, and μ. Both α, β are free parameters with $0 \leqslant \alpha, \; \beta \leqslant \infty$. Rate functions $f(N)$ and $g(N)$ control the actual entry and exit of particles to and from T. Since we are considering a situation where enhanced particle content in R leads to a greater inflow of particles into T and hinders outflow of particles from T to R, $f(N)$ and $g(N)$ are assumed to be, respectively, monotonically increasing and

decreasing functions of N. Once the functions $f(N)$ and $g(N)$ are specified, our model is completely defined.

This model can be studied for specific independent choices of $f(N)$ and $g(N)$, subject to the general condition that in order to reflect the crowding effect in a meaningful way $f(N)$ and $g(N)$ should be, respectively, increasing and decreasing functions of N. We intend to study the effects of coupling f and g that can arise through their dependence on a common quantity N. Given their monotonic nature of dependences on N and positive definiteness, their mutual coupling should be such that when one of them increases, the other should decrease. While there can be many different choices of couplings between $f(N)$ and $g(N)$, in the present work, we choose a very simple form of the coupling by setting

$$f(N) + g(N) = 1. \tag{2}$$

This choice clearly ensures that when f rises, g decreases, and vice versa. In order to be able to proceed further, we make the choice $f(N) = N/N^*$, for reasons of analytical amenability, where N^* is a scale that sets the capacity of the reservoir; see also Ref. [7]. The steady states should depend on what we choose for N^*. In the absence of any general results, it is useful to consider specific simple choices for N^*. In this work, we focus on the specific case where $N^* \equiv N_0$, the total available particles. This corresponds to a situation where all the particles in the system can be accommodated in the reservoir; this means the total particle number in TASEP can never exceed N^*. This gives

$$f(N) = N/N_0. \tag{3}$$

The choice (3) implies that the actual entry rate is proportional to the reservoir occupation N. Thus, $f(N)$ rises monotonically with N with $f(0) = 0$ and $f(N = N_0) = 1$. The choice (3), though similar, but is different quantitatively from the existing models for TASEPs with finite resources [4–7]; this suffices for our purposes and is easily amenable to analytical MFT treatments. Further, the choice (3) implies

$$g(N) = 1 - f(N) = 1 - N/N_0. \tag{4}$$

Thus, $g(N)$ is monotonically decreasing with the reservoir occupation N with $g(0) = 1$ and $g(N = N_0) = 0$. We thus see that as N rises, $f(N)$ rises but $g(N)$ reduces. This implies that as N increases, more particles try to enter into the TASEP lane and fewer particles would be able to leave it. In particular, for large N_0, when most of the particles are in R, α_e approaches α and β_e becomes very small. On the other hand, for small N_0, when the reservoir population N is also small, α_e is small, but β_e approaches β. Thus, fewer particles will enter T, but those which are already in T have a larger tendency to leave T and to enter R. These features form the essence of the crowding effect that we intend to study and distinguish our model from the existing models for TASEPs with finite resources where the exit rates are a free model parameter (just as in open TASEPs) [4–8]. Our choices (3) and (4) are simple and minimal choices that are easily analytically tractable and suffice to study the crowding effect introduced above. Since the only condition on $f(N)$ and $g(N)$ is that these functions must be non-negative, N can go up to N_0. Since N_0, the total number of particles, can even be infinity, there are no restrictions on N either.

III. STEADY-STATE DENSITIES

Let n_i be the occupation at site i and J be the corresponding current. The latter is a constant in the steady states. Below we outline the mean-field theory (MFT) and use it to obtain the phases and phase diagram in the α-β plane, parametrized by μ, supported by our extensive MCS studies. Before we embark on our MFT analysis, we already note that for small μ, α_e should be small, whereas β_e should be large. Thus T should not be in its HD phase. In fact, if $\mu < 1/2$, there are not enough particles in the system to keep T in its HD or MC phases. Thus, for $\mu < 1/2$, T is *always* in its LD or SP phases independent of α and β. In contrast, for very large μ, $\alpha_e \gg \beta_e$ and T are expected to be in the HD phase only. For intermediate values of μ, transition to the MC phase may be observed. We will see below that our detailed MFT analysis corroborates this intuitive physical picture.

We first summarize our results in terms of a series of phase diagrams in the α-β plane parametrized by $\mu = 0.6,\ 1,\ 2,\ 1000,\ 100\,000$; see Fig. 2(a), Fig. 2(b), Fig. 2(c), Fig. 2(d), and Fig. 2(e), respectively. As revealed by these phase diagrams, the phases and the phase boundaries in the α-β plane sensitively depend upon the value of μ.

Direct visual inspections of these phase diagrams reveal the following qualitative features. There are four phases, LD, HD, MC, and SP, in these phase diagrams. Further, all the phase boundaries meet at a single point. Then at $\mu = 1$ all the phase boundaries are straight lines, whereas for all $\mu \neq 1$, except for the SP-HD boundary, all other boundaries are again straight lines. In contrast, the SP-HD boundary is a curved line for $\mu \neq 1$, whose shape appears to change as μ crosses unity. The phase diagrams in Fig. 2(c) ($\mu = 2$), Fig. 2(d) ($\mu = 1000$), and Fig. 2(e) ($\mu = 100\,000$) have very similar forms; however, the scales of the β-axis in these figures differ enormously. We now discuss the principles behind calculating these phase boundaries and the phase diagrams.

IV. MEAN-FIELD THEORY

We now use MFT to construct the principles behind obtaining the phase diagrams and the associated density profiles in the steady states. We recall that the instantaneous configuration of T, having L sites, is described by a set of occupation numbers that can take values 0 or 1, for each of the sites in T. MFT entails neglecting spatial correlations: $\langle \rho_i \rho_{i=1} \rangle \approx \langle \rho_i \rangle \langle \rho_{i+1} \rangle$, where ρ_i is the occupation at site i and $\langle \cdots \rangle$ implies averages in the steady states. One then takes the continuum limit with $\rho(x) \equiv \langle n(i) \rangle$, denoting the steady-state densities in T; $x = i/L$ becomes quasicontinuous in the thermodynamic limit $L \to \infty$ [15,16]. Here x starts from 0 at the entry end with $x = 1$ at the exit end. MFT applications have a long history in TASEP. It was first used for a single TASEP lane with open boundaries, which was later corroborated by more sophisticated arguments [17]. Later, MFT has been widely applied in many different variants of TASEP; see, e.g., Refs. [7,8,14,18–22], with strong validation from stochastic simulations of the microscopic models. In the absence of any rigorous proof available for the validity of MFT in TASEPs with fixed resources, we use it as a guideline to understand the broad features of the consequences of the dynamically coupled rates introduced here, which are complemented and

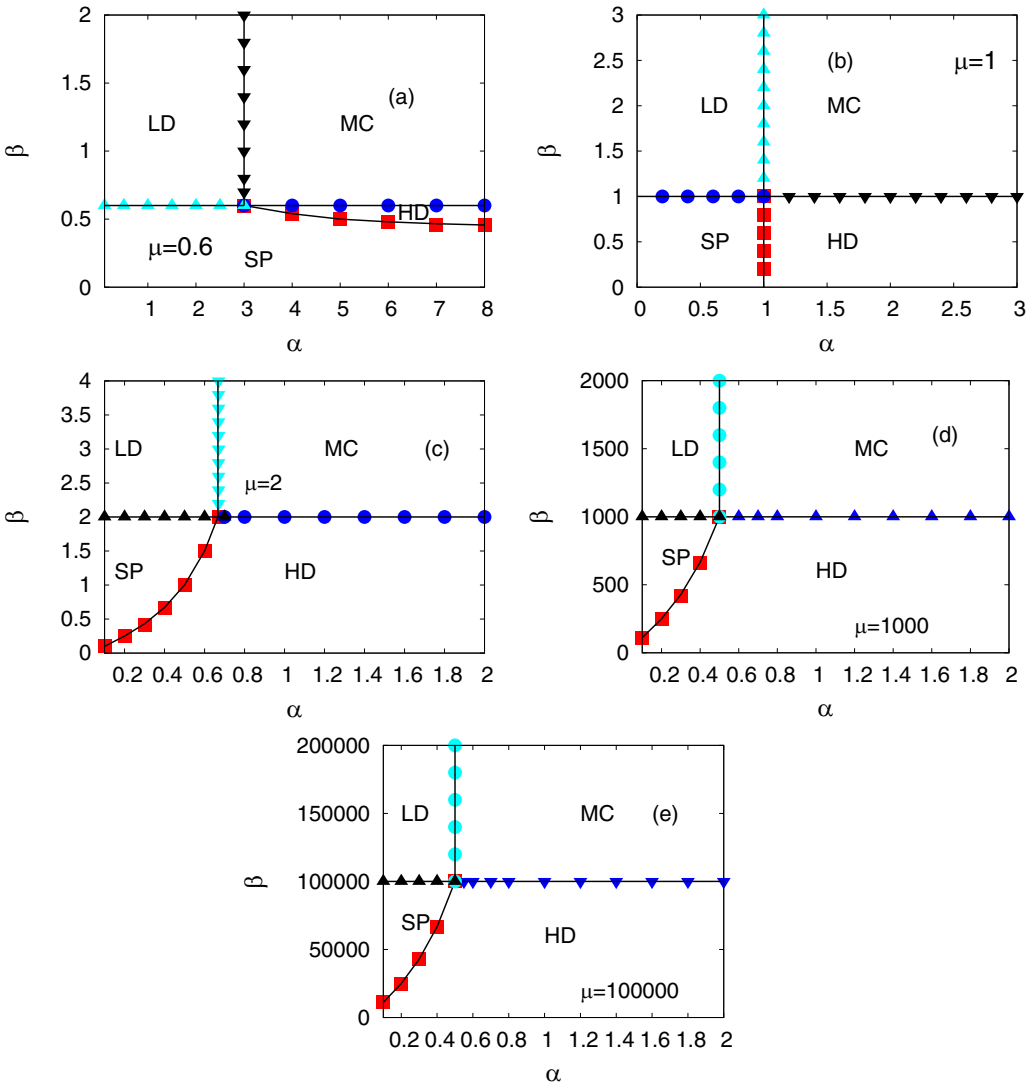

FIG. 2. Phase diagrams in the α-β plane. (a) $\mu = 0.6$, (b) $\mu = 1$, (c) $\mu = 2$, (d) $\mu = 1000$, (e) $\mu = 100\,000$. Continuous lines represent the MFT predictions (see text); the discrete points are the corresponding MCS results, which agree well with the MFT predictions.

supported by our MCS studies. The latter undoubtedly lends credence to the MFT applications in the present model. In our MFT analysis, we study the phases of T in terms of the well-known phases of a TASEP lane with open boundaries, delineated by the effective entry (α_e) and exit (β_e) rates, respectively [7,8,14,18]. In the next sections, we obtain the phase boundaries in α-β plane, parametrized by μ, and the corresponding steady-state densities in the different phases.

A. Low-density phase

We begin with the LD phase. In the LD phase, we get by using (3)

$$\rho_{LD} = \alpha_e = \alpha \frac{N}{N_0}. \tag{5}$$

The total particle number is given by $N_0 = N + L\alpha_e$. This implies for the total particle number

$$N_0 = N\left(1 + \frac{\alpha L}{N_0}\right). \tag{6}$$

This then gives

$$\rho_{LD} = \frac{\alpha}{1 + \frac{\alpha}{\mu}}, \tag{7}$$

giving $\rho_{LD} < \alpha$, as expected. See Fig. 3 for representative plots of the steady-state density profiles in the LD phase with different parameter values: $\mu = 1000$, $\alpha = 0.2$, and $\beta = 1500$, and $\mu = 1$, $\alpha = 1/2$, and $\beta = 2$.

From Eq. (7), we note that as μ grows, ρ_{LD} approaches α as it would be for an open TASEP (for $\alpha < 1/2$); see Fig. 4.

B. High-density phase

Proceeding similarly for HD phase, we find

$$\rho_{HD} = 1 - \beta + \frac{\beta\left(1 - \frac{1-\beta}{\mu}\right)}{1 + \frac{\beta}{\mu}} = \frac{\mu}{\beta + \mu}. \tag{8}$$

Thus, ρ_{HD} can be more or less than $1 - \beta$, the HD phase bulk density in an open TASEP with an exit rate β. See Fig. 5

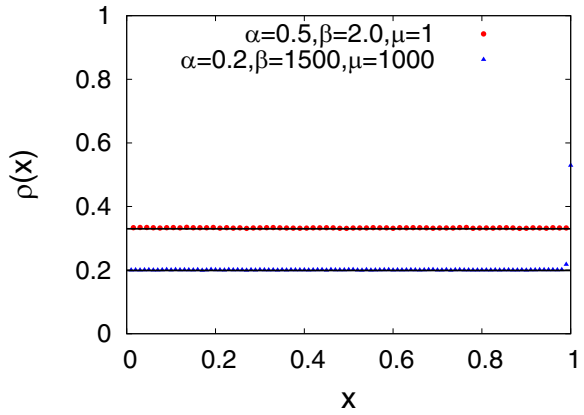

FIG. 3. Plots of $\rho(x)$ in the LD phase with different values for the parameters: $\mu = 1000, \alpha = 0.2$, and $\beta = 1500$, and $\mu = 1, \alpha = 1/2$, and $\beta = 2$. Continuous lines represents the MFT predictions (see text), discrete points are the corresponding MCS results. Very good agreements between the MFT and MCS predictions are found. Notice that for $\mu = 1000$, bulk density ρ_{LD} is very close to α, whereas for μ, it is substantially less than α (see text). Unsurprisingly, ρ_{LD} is independent of β.

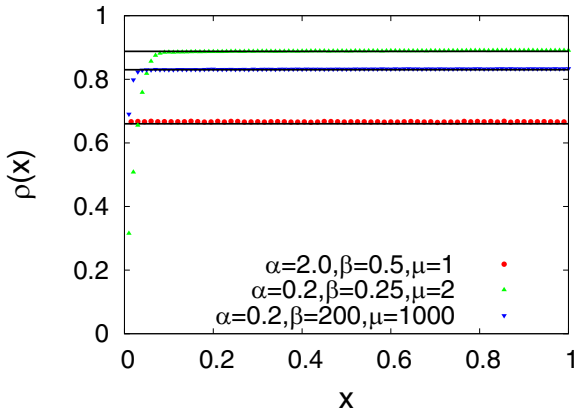

FIG. 5. Plots of $\rho(x)$ in the HD phase for $\mu = 2$, $\alpha = 0.2$ and $\beta = 0.25$, and $\mu = 1000$, $\alpha = 0.2$, and $\beta = 200$, and $\mu = 1$, $\alpha = 2$, and $\beta = 1/2$. Continuous lines represent the MFT predictions (see text); discrete points are the corresponding MCS results. Very good agreements between the MFT and MCS predictions are found. Notice that ρ_{HD} can be both smaller or larger than $1 - \beta$ (see text). Unsurprisingly, ρ_{HD} is independent of α.

with ($\mu = 2$, $\alpha = 0.2$, and $\beta = 0.25$), ($\mu = 1000$, $\alpha = 0.2$, and $\beta = 200$), and ($\mu = 1000$, $\alpha = 0.2$, and $\beta = 200$).

As revealed by Eq. (8), ρ_{HD} approaches *unity* (and hence independent of β) as μ becomes large; see Fig. 6. This is in contrast with and marks a significantly departure from an open TASEP.

C. Maximal current phase

The MC phase is characterized by $\rho(x) = 1/2$ in the bulk as shown in Fig. 7. Hence, at the transition between LD to MC phase $\rho_{LD} = \frac{1}{2}$. This gives the condition

$$\alpha = \frac{1}{2 - \frac{1}{\mu}}. \tag{9}$$

Since $\alpha > 0$ by definition, μ must be larger than $1/2$ for the boundary (9) to exist. In fact, there is *no* MC phase if $\mu < 1/2$, in agreement with our heuristic argument above. Notice that the boundary (9) between the LD and MC phases is independent of β, and hence parallel to the β-axis in the α-β plane; see the phase diagrams in Fig. 2, as obtained from our MFT as well as our MCS simulation studies.

Similarly, at the transition between HD to MC phase, one has $\rho_{HD} = \frac{1}{2}$, which in turn gives

$$\beta = \mu. \tag{10}$$

The boundary (10) between the HD and MC phases is again a straight line in the α-β plane, in this case parallel to the α-axis, as can be seen in the phase diagrams in Fig. 2.

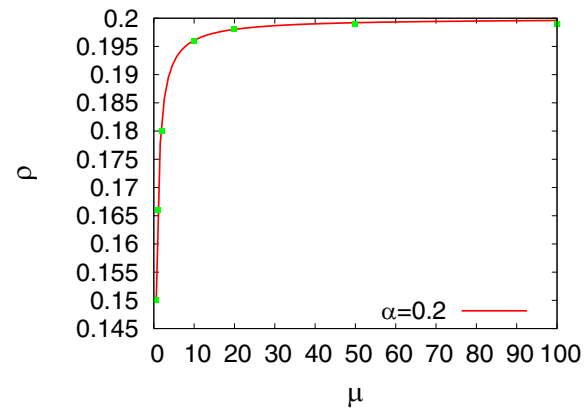

FIG. 4. Plot of ρ_{LD} vs μ for a given $\alpha = 0.2$. The continuous black line represents the MFT result given by Eq. (7); the points represent the MCS data. Clearly ρ_{LD} approaches α as μ grows (see text). Very good agreements between the MFT and MCS predictions are found.

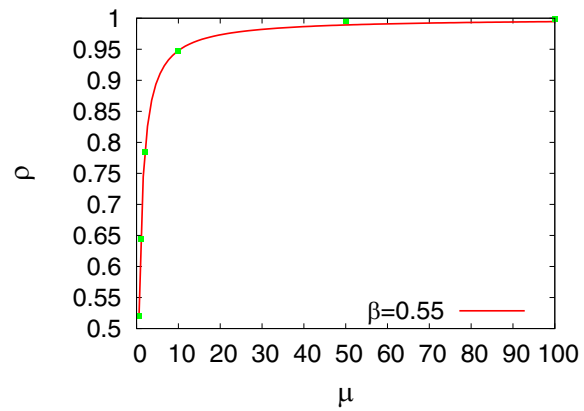

FIG. 6. Plot of ρ_{HD} versus μ for given $\beta = 0.55$. The continuous line represents the MFT result given by Eq. (8); the points represent the MCS data. Clearly, ρ_{HD} approaches unity as μ becomes large (see text). Very good agreement between MFT and MCS results are found.

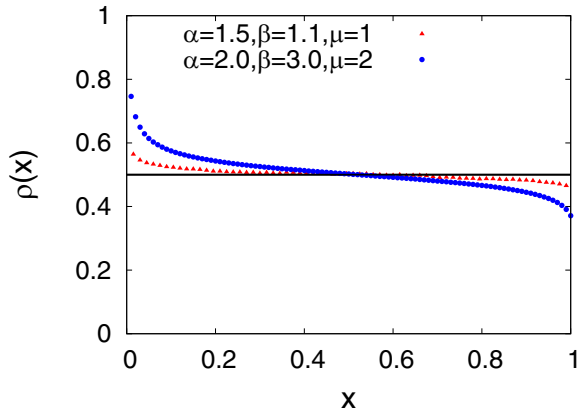

FIG. 7. Plots of $\rho(x)$ in the MC phase for $\mu = 1$, $\alpha = 1.5$, and $\beta = 1.1$, and $\mu = 2$, $\alpha = 2.0$, and $\beta = 3.0$. Continuous black lines represent the MFT predictions (see text); discrete points are the corresponding MCS results. Good agreements between the MFT and MCS predictions are found. Unsurprisingly, the bulk density (=1/2) is independent of α, β; the deviations from 1/2 near the boundaries are the boundary layers that exist even in open TASEPs.

D. Shock phase and domain walls

The transition between the LD and the HD phases is marked by the condition

$$\rho_{LD} + \rho_{HD} = 1, \tag{11}$$

which is equivalent to $\alpha_e = \beta_e$. In open TASEPs, this transition is marked by a single delocalized domain wall (DDW) that spans the whole length of the TASEP. This is usually attributed to uncorrelated entry and exit events in an open TASEP. In the present model, there is a strict number conservation. This leads to a localized domain wall (LDW), as opposed to a DDW in an open TASEP [14,18]. Similar LDWs or pinning of domain walls were found in previous studies on TASEPs with fixed resources, where the exit rates were taken to be constants [4–8]. We discuss the principle behind the formation of these domain walls and their pinning below; see also Refs. [4–8].

In order to characterize the SP fully, we must obtain the domain wall height Δ and the domain wall position x_w as functions of the model parameters. From particle number conservation, we get

$$N_0 = L\int_0^1 \rho(x)\,dx + N. \tag{12}$$

This implies

$$\begin{aligned}\mu &= \int_0^{x_w} dx\,\alpha_e + \int_{x_w}^1 (1-\beta_e)\,dx + N/L \\ &= \alpha_e x_w + (1-\beta_e)(1-x_w) + N/L \\ &= \frac{N\alpha}{N_0}x_w + 1 - x_w - \beta\left(1-\frac{N}{N_0}\right) \\ &\quad + \beta\left(1-\frac{N}{N_0}\right)x_w + \frac{N}{L}.\end{aligned} \tag{13}$$

At the LD-HD coexistence, we have

$$\alpha_e = \beta_e. \tag{14}$$

This gives

$$\begin{aligned}\alpha\frac{N}{N_0} &= \beta\left(1-\frac{N}{N_0}\right), \\ \Rightarrow (\alpha+\beta)\frac{N}{N_0} &= \beta, \\ \Rightarrow \frac{N}{N_0} &= \frac{\beta}{\alpha+\beta}.\end{aligned} \tag{15}$$

Thus, N/N_0 is *independent* of μ. Hence,

$$\alpha_e = \frac{\alpha\beta}{\alpha+\beta} = \beta_e. \tag{16}$$

Using the above equation in (13) for μ we write

$$\begin{aligned}\mu &= x_w\alpha\frac{\beta}{\alpha+\beta} + 1 - x_w - \beta + \beta\frac{\beta}{\alpha+\beta} \\ &\quad + \beta x_w - x_w\beta\frac{\beta}{\alpha+\beta} + \mu\frac{\beta}{\alpha+\beta}.\end{aligned} \tag{17}$$

Simplifying the above equation we get

$$x_w = \frac{\mu\alpha - \alpha - \beta + \alpha\beta}{2\alpha\beta - \alpha - \beta}. \tag{18}$$

This gives the position of DW. Note that for fixed α, β, x_w changes continuously with μ. For the SP phase to exist, $0 < x_w < 1$. For HD to SP transition $x_w = 0$, which in turn implies

$$\beta = \frac{\alpha(\mu-1)}{1-\alpha}. \tag{19}$$

For LD to SP transition $x_w = 1$, which implies

$$\beta = \mu. \tag{20}$$

In the α-β plane, (19) is clearly not a straight line in general, where (20) is a straight line. See the phase diagrams in Fig. 2. For $\mu = 1$, the phase boundary is, however, a straight line; see Fig. 2(b). The SP phase is thus confined between the lines (20) and (19), and hence covers *a region* in the α-β plane.

We now find the height of the domain wall. Noting that at the entry side, $\rho(x)$ has a mean value $\rho_{LD} = \alpha_e$, whereas on the exit side, $\rho_{HD} = 1 - \beta_e = 1 - \alpha_e$, since $\alpha_e = \beta_e$ for a domain wall to exist, we find the domain wall height Δ as

$$\Delta = \rho_{HD} - \rho_{LD} = 1 - 2\alpha_e = 1 - 2\frac{\alpha\beta}{\alpha+\beta}. \tag{21}$$

See Fig. 8 for plots of LDW for various values of the model parameters.

It is clear from these figures that the LDW height Δ is a function of α, β, but does not depend upon μ [cf. Eq. (21); see also Fig. 9]. In contrast, its position x_w depends on all three of α, β, and μ [cf. Eq. (18)]. In fact, from Eq. (18), we note that if $\alpha = 1/2$, $x_w = \beta - (\mu - 1)$, a straight line as a function of β, but is a generic nonlinear function of β for all other values of α; x_w retains a linear dependence on μ for all α, β within SP.

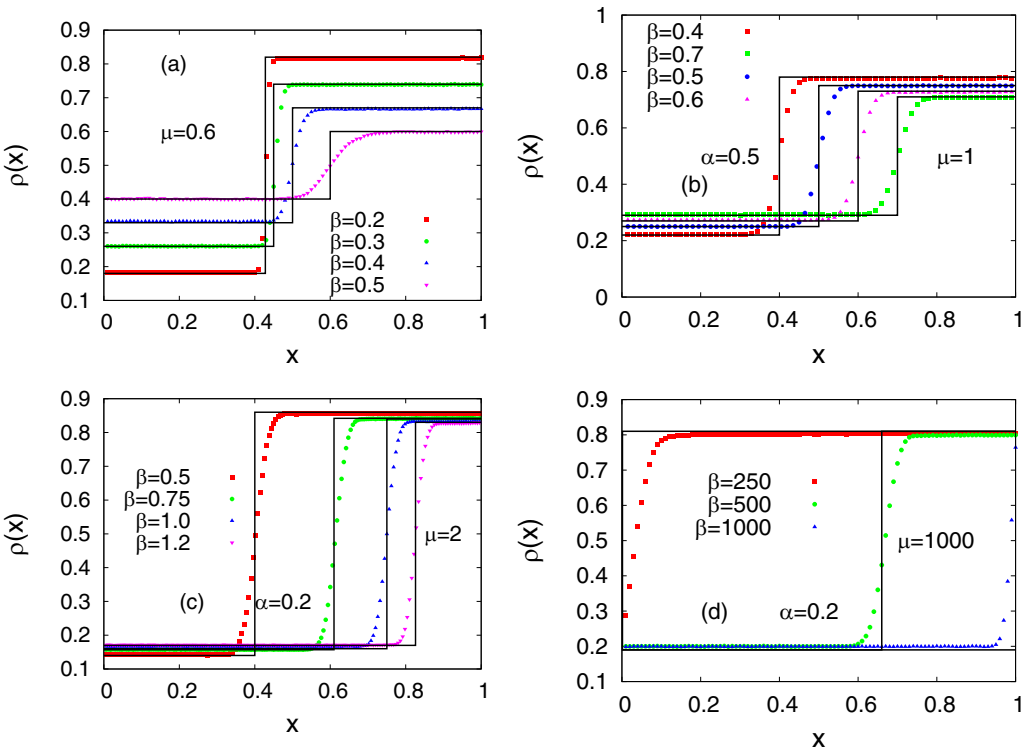

FIG. 8. LDW in T for different values of β with (a) $\mu = 0.6, \alpha = 2.0$, (b) $\mu = 1, \alpha = 0.5$, (c) $\mu = 2, \alpha = 0.2$, and (d) $\mu = 1000, \alpha = 0.2$. Continuous black line represents the MFT prediction (see text), points in various colors are the corresponding MCS results.

In Fig. 10 and Fig. 11, we have shown the dependence of x_w and Δ on β for given α, μ, as obtained from our MFT and MCS studies.

The reason that Δ is independent of μ lies in Eq. (15), which shows that the reservoir occupation N *does not* depend upon μ in the SP phase. Thus, as μ is varied within the SP phase, N does not change; as a result α_e and β_e do not change which in turn leaves Δ unchanged. As μ changes N_0, however, changes. These extra or deficit particles are adjusted by changing the position x_w of the DW [23].

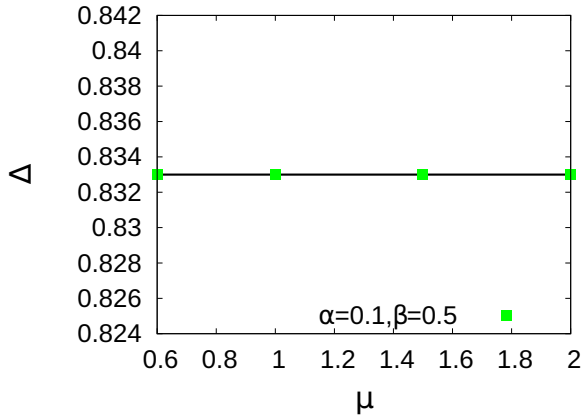

FIG. 9. Plot of Δ vs μ for $\alpha = 0.1$, $\beta = 0.5$. The continuous line represents the MFT result for Δ given by Eq. (21); the discrete points are the corresponding MCS results. Very good agreements between MFT and MCS results can be seen. Clearly, Δ does not depend on μ within SP (see text).

E. Phase boundaries meet a common point

All four phase boundaries meet at a common point $(\alpha_c, \beta_c) = (\mu/(2\mu - 1), \mu)$, which is a *multicritical point*, as we explain below in the next section. It is, however, useful to consider the "distance" d between the origin (0, 0) and (α_c, β_c) as a function of μ: We find

$$d = \sqrt{\frac{\mu^2}{(2\mu - 1)^2} + \mu^2}. \tag{22}$$

Thus, d diverges when $\mu \to 1/2$ from above, or when $\mu \to \infty$; see Fig. 12 for a plot of $d(\mu)$ versus μ. Both MFT and MCS results are shown, which agree well with each other.

In the limit of infinite capacity, i.e., $\mu \to \infty$, $(\alpha_c, \beta_c) \to (1/2, \infty)$. Since $\beta_c \to \infty$, the latter phase essentially is confined to the β-axis (see Sec. IV F). On the other hand, as $\mu \to 1/2_+$, $(\alpha_c, \beta_c) \to (\infty, 1/2)$. Thus, for $\beta < 1/2$ and all α, the TASEP shows an LDW, whereas for $\beta > 1/2$ and all α, the system is in the LD phase. For $\mu < 1/2$, α_c becomes negative, which is unphysical. As heuristically argued above, this implies that for $\mu < 1/2$, the system can only be in the LD phase or SP, as there are not enough particles for HD or MC phases. This can be understood easily. Since HD or MC phase would require at least $\mu = 1/2$ or more (assuming all particles are in T, leaving the reservoir empty), with $\mu < 1/2$, there are enough particles just for LD and SP only.

The nature of the HD-SP boundary changes as μ crosses unity, as is evident from Eq. (19). For $\mu < 1$, $\alpha > 1$ necessarily. On the boundary, as α (> 1) grows, β decreases. In fact, in the limit $\alpha \to \infty$, $\beta \to 1 - \mu$. In contrast for $\mu > 1$, $\alpha < 1$ at the boundary since β cannot be negative. As $\alpha (< 1)$ reduces,

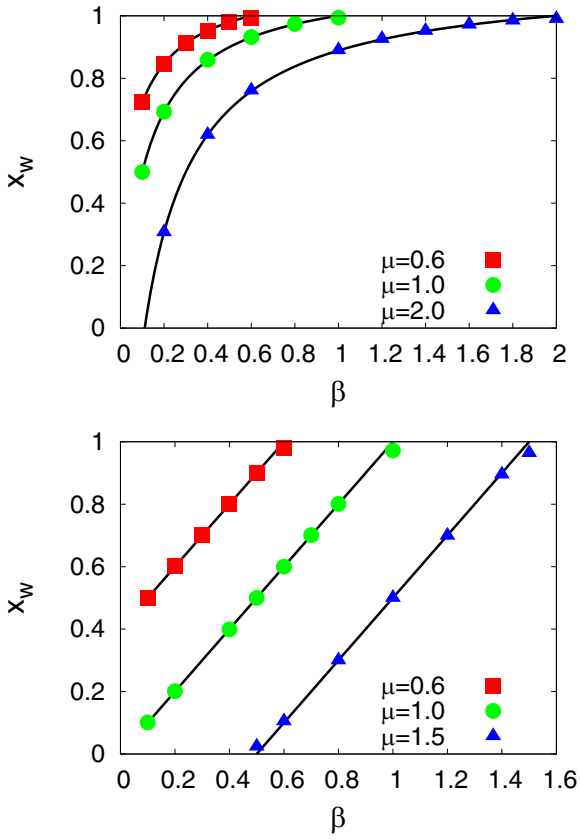

FIG. 10. Plot of x_w versus β for (top) $\alpha = 0.1$ and (bottom) $\alpha = 0.5$. The continuous line represents the MFT result for x_w given by Eq. (18); the discrete points are the corresponding MCS results. For $\alpha = 0.1$, the dependence of x_w on β is not linear, whereas for $\alpha = 0.5$, it depends linearly (see text). Very good agreements between MFT and MCS results can be seen.

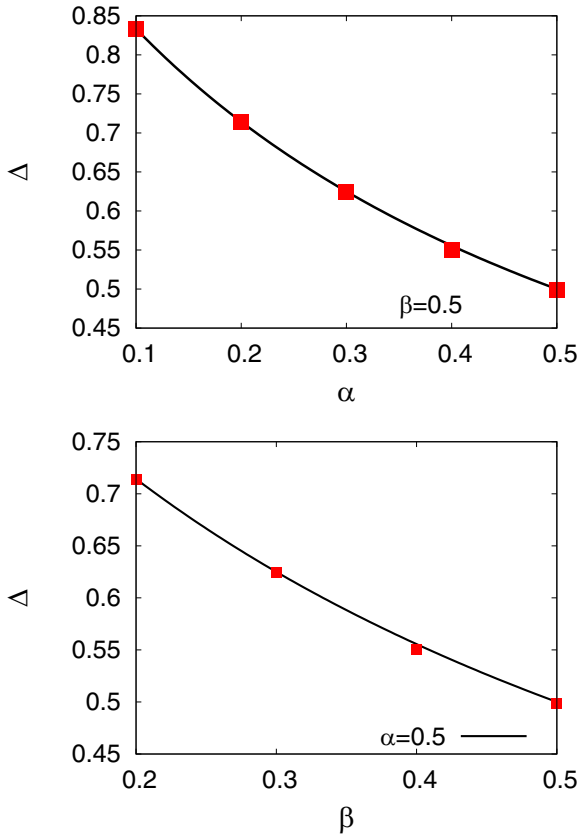

FIG. 11. Plot of Δ (top) versus α for $\beta = 0.5$ and $\mu = 0.6$ and $\mu = 1$, (bottom) vs β for $\alpha = 0.5$ and $\mu = 0.6$ and $\mu = 1$. The continuous line represents the MFT result for Δ given by Eq. (21); the points represent the corresponding MCS results, which overlap. Very good agreements between the MFT and MCS results can be seen.

β also reduces. This explains the difference between the shape of the HD-SP boundary in Fig. 2(a) ($\mu = 0.6 < 1$) *vis-à-vis* in the other phase diagrams in Fig. 2 with $\mu > 1$. The phase diagram in Fig. 2(b) for $\mu = 1$ merits separate attention. At $\mu = 1$, (18) gives $\alpha = 1$ as the boundary between the HD and SP (since $\beta \neq 0$). On the other hand, (20) gives $\beta = 1$ as the boundary between LD and SP for $\mu = 1$. With $\mu = 1$, all the four phases meet at (1, 1) in the α-β plane. This immediately gives the phase diagram in Fig. 2(b).

F. Phases for infinite resources

We now find out the steady states with infinite resources, i.e., diverging N_0. This limit can be reached in two ways. For instance, we could take the limit $N_0 \to \infty$, keeping the ratio N/N_0 fixed. This implies a fixed ρ/μ, where ρ is the mean TASEP density. Now, for a fixed N/N_0, functions $f(N)$ and $g(N)$ do not change, and hence, for fixed α, β, ρ too remains unchanged. Thus, in this way of taking the limit $N_0 \to \infty$, μ in turn remains fixed. This is equivalent to making the size L of the TASEP lane scaling with N_0. In this case, α_e and β_e remain fixed. Therefore, the steady-state density of the TASEP lane too remains unchanged. Alternatively, one could take the limit $N_0 \to \infty$ keeping L fixed, a situation mentioned in Refs. [7,8]. In this case, $N_0 \to \infty$ implies $\mu \to \infty$. In this case, α_e and β_e are expected to change. By using the logic of the MFT constructed above, we can now infer the admissible phases for $\mu \to \infty$. When $\mu \to \infty$, the reservoir occupation N must also approach infinity, since almost every particle will be in R in that limit. In the same limit of the existing models for TASEPs with finite resources, the phase diagrams in the plane of the parameters equivalent to α, β here approach that for a single open TASEP; see, e.g., Refs. [7,8]. In our model, as μ rises, the region of the phase space spanned by the HD phase rises, a feature that is evident from the phase diagrams presented above. Due to the crowding effect modeled here by (2), $\beta_e \to 0$ and $\rho_{HD} \to 1$ for any finite α; see Eq. (8). Thus the TASEP channel should be nearly filled, with the HD phase being the only possible phase for any finite α and β. No other phase is to be observed, including no possibility of any domain wall for any finite α and β. This makes it significantly different from an open TASEP which can be in LD, HD, or MC phases. That only the HD phase is possible can be seen from the fact that the multicritical point (α_c, β_c) moves to $(1/2, \infty)$ for $\mu \to \infty$. Thus the boundaries between the SP and LD phases and HD and MC phases all move to $\beta = \infty$. Further, the slope of the boundary between the SP and HD phases, as given by Eq. (19), diverges as $\mu \to \infty$, indicating that the shock phase essentially gets concentrated

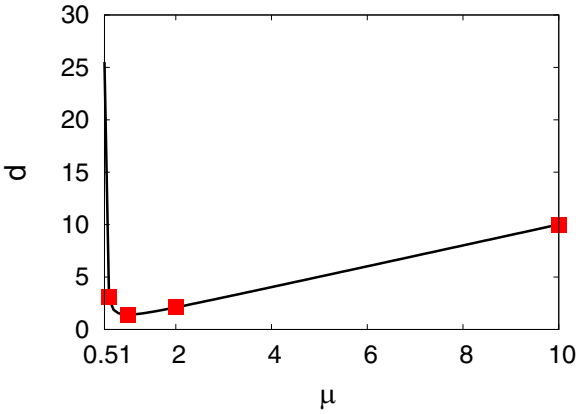

FIG. 12. Plot of $d(\mu)$ vs μ in the SP phase. The continuous line represents the MFT result given by Eq. (22); the discrete points are the corresponding MCS results. Clearly d diverges for when either $\mu \to 1/2$, or $\mu \to \infty$, showing the absence of the four-phase coexistence point as these two limits are approached (see text). Very good agreement between MFT and MCS results is found.

on the β-axis, leaving the entire phase diagram to be spanned by the HD phase for any finite α and β. This is clearly in contrast to the existing models and is essentially an outcome of the reservoir population-dependent coupling between the effective entry and exit rates.

V. PHASE TRANSITIONS IN THE MODEL

Phase diagrams in Fig. 2 all have different phases separated by sharp phase boundaries. We now discuss the nature of the transitions across these phase boundaries. In an open TASEP, the transitions between the LD and HD phases are accompanied by a sudden jump in the bulk density in the TASEP, which indicates a first-order transition with the steady-state bulk density acting as the order parameter. The corresponding phase boundary is characterized by a single DDW. In the same vein, the transitions between the LD or HD and MC phases are second-order transitions, with the density changing smoothly at the phase transition. In the phase diagram of an open TASEP, three phase boundaries—two second-order (LD-MC and HD-MC) and one first-order (LD-HD) boundary—meet at a multicritical point. In contrast, the phase diagrams for the present model generically all have four phase boundaries, one each for the transition between LD-MC, LD-SP, MC-HD, and SP-HD phases. Notice that, unlike for an open TASEP, there is *no* phase boundary that acts as the boundary between the LD and HD phases. In other words, as one moves in the parameter space, one cannot directly move from the LD to the HD phases and vice versa. Again taking the steady-state bulk density as the order parameter, we note that the density changes *smoothly* across all four phase boundaries. Thus, all the transitions and the associated phase boundaries represent *second-order* transitions. This can be easily seen in Fig. 13, where we have plotted the mean density (a) ρ_α as a function of α for a fixed β and μ, and (b) ρ_β as a function of β for a fixed α and μ. In Fig. 13(a) the values of $\rho_\alpha(\beta = 1)$ in their SP phases are calculated from the respective density profiles by using (18) and (21) for given α, β, and μ, and then averaging

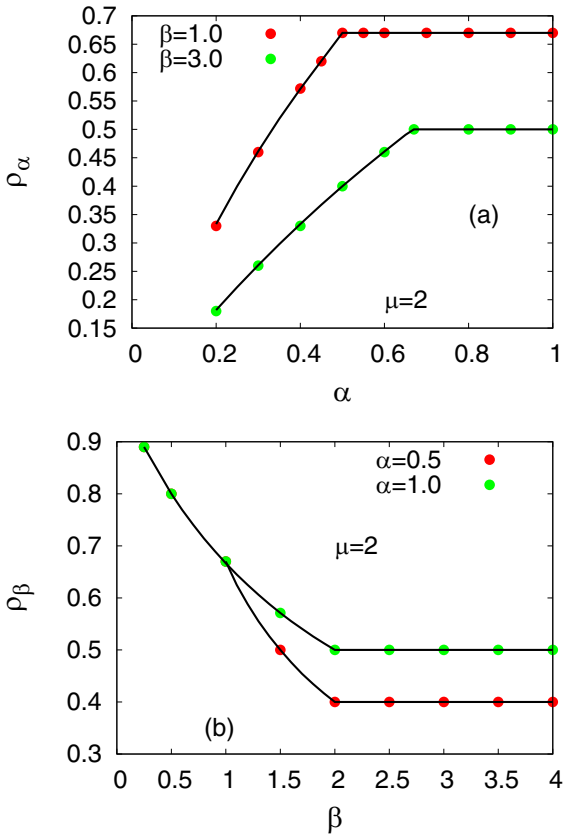

FIG. 13. Plots of the mean density as a function of (a) α for fixed $\beta = 1, 3$, and $\mu = 2$, and (b) β for fixed $\alpha = 1/2, 1$ and $\mu = 2$. In (a) ρ changes smoothly from SP to HD ($\beta = 3$) with ρ becoming independent of α, and LD to MC ($\beta = 1$) with $\rho = 1/2$. In (b) ρ changes smoothly from HD to MC ($\alpha = 1$) with $\rho = 1/2$, and SP to LD ($\alpha = 1/2$) with ρ becoming independent of β. MFT (lines) and MCS (points) are shown, which show good agreement; see text. MFT (continuous lines) and MCS (discrete points) show very good agreement.

over the system, which matches smoothly the corresponding bulk density in the HD phase that is independent of α as given by (8) and the LD phases values (7) of $\rho_\alpha(\beta = 3)$ match smoothly with its MC phase value (=1/2). Likewise in Fig. 13(b) the values of ρ_β ($\alpha = 0.5$) in their SP phases match smoothly with the corresponding LD phase values given by (7) and ρ_β ($\alpha = 1$) in HD phases matching smoothly the MC phase. These clearly demonstrate smooth changes in the mean density across the phase transitions.

All these four second-order lines meet at a multicritical point (α_c, β_c). This feature of the phase diagram is similar to that in the model studied in Refs. [8,18], and in one of the models studied in Refs. [14]. Last, for $\mu < 1/2$, there are only two phases—LD and SP—possible, and the multicritical point naturally ceases to exist for $\mu < 1/2$.

VI. NATURE OF THE DOMAIN WALLS

As a consequence of the strict particle number conservation, MFT gives the precise location of the DW [see Eq. (18)], implying an LDW; see Fig. 8 for representative plots of LDW for various values of the model parameters. It is clear that the

domain wall is *always* sharply pinned for all the choices of μ. This is in contrast to a DDW in an open TASEP that has no particle number conservation in it. Still, the LDW does fluctuate about its mean position, as the particle number conservation applies on the whole system, and not on the TASEP segment, leaving the particle content in the TASEP to fluctuate (subject to maintaining the overall conservation). Indeed, it was shown recently [14] that in a ring geometry consisting of a TASEP segment and a diffusive segment, in certain limits of the model parameters when the variance of the TASEP particle content scales with the size of the TASEP or the relative particle content of the diffusive segment, the LDW gets depinned and takes a form identical to that of a DDW in an open TASEP. This was explained in terms of the attendant diverging particle fluctuations in the TASEP segment necessary for the formation of a DDW [14]. It was further demonstrated that this transition from an LDW to a DDW is a smooth crossover with the LDW fluctuations increase gradually with the extent of particle number fluctuations in the TASEP segment, which in turn grows with the size of the diffusive segment, or the relative particle content of the diffusive segment. Analogous to the studies in Ref. [14], it is expected that with rising μ, i.e., with increasing total particle numbers in the system, the LDW fluctuations should increase leading to its eventual delocalization and formation of a DDW. Surprisingly and unexpectedly, no such tendency towards eventual delocalization of the LDW has been observed in the MCS studies of the present model. We now explain this unexpected lack of delocalization by systematically studying its fluctuations.

To proceed further, we need to go beyond the MFT description developed above, and we now analyze the domain wall fluctuations. For this, we closely follow Refs. [19,22] in this section. We consider a domain wall with a position at x_w, that fluctuates in time. With Δ as the height of the DW, increasing the number of particles by one implies shifting the instantaneous DW by $\delta x_w = -1/(L\Delta)$. Similarly, a particle exiting the TASEP means shifting the DW by $\delta x_w = +1/(L\Delta)$. Let $P(x_w, t)$ be the probability of finding the DW at x_w at time t. Then, following Refs. [19,22], we find that P satisfies the Fokker-Planck equation

$$\frac{\partial P}{\partial t} = D\frac{\partial^2}{\partial y^2}P, \tag{23}$$

where $y \equiv \delta x_w$ and D is a diffusion constant given by

$$D = \tfrac{1}{2}[\alpha_e(1-\alpha_e) + \beta_e(1-\beta_e)]. \tag{24}$$

As shown above, in the limit $\mu \to \infty$, $1-\beta_e = \rho_{HD} \to 1$. This implies $\beta_e \to 0$. Since $\alpha_e = \beta_e$ for a DW, we must have $\alpha_e \to 0$ as well. Thus, $D \to 0$ for $\mu \to \infty$. Therefore, the corresponding timescale of fluctuations $1/D$ diverges for a fixed L. Thus, even for a finite L, the typical time required for the DW to traverse the whole of TASEP of size L diverges, making any delocalization essentially unobservable.

VII. SUMMARY AND OUTLOOK

In this article, we have explored the "crowding effect" of the reservoir on the attached TASEP within a simple model, that to our knowledge has previously not been investigated. To this end, we have studied the nonequilibrium steady states of a TASEP connected at both its ends to a reservoir without any internal dynamics. Both the effective entry and exit rates to and from the TASEP, respectively, depend on the reservoir occupation number, that in turn creates a dynamical coupling between the two rates, a key ingredient of our model. The dynamically controlled effective rates ensure that a rising reservoir occupation can hinder flow of particles from TASEP back to the reservoir, but facilitates particle flow into TASEP and vice versa, a property that we have named the "crowding effect" of the reservoir. We have focused on how the total particle number conservation conspires with the crowding effect to ultimately control the steady-state density profiles and the phase diagram of the TASEP. This model generically shows a static or pinned domain wall or a single LDW, unlike for an open TASEP. Furthermore, the *shock phase*, where such an LDW is expected to be observed, is no longer a single line as for an open TASEP, but rather covers a *region* in the parameter space spanned by the two entry and exit rate parameters. As a result, all the transitions in this model are *second order* in nature. The LDW, rather unexpectedly, does not show any tendency to delocalize even for large resources, in contrast to the results of Ref. [14]. This is explained as a consequence of the form of the dynamic coupling between the entry and exit rate. While it is naïvely expected that in the limit of a very large particle number, this model should reduce to an open TASEP, for in that limit, the effects of particle number conservation should not be relevant, and we show that it does not happen: the large density limit of this model is *distinct* from an open TASEP, as it still allows only an LDW and not a DDW. This is primarily a consequence of the crowding effect, as argued here, which is never present in an open TASEP. We have used analytical MFT and MCS studies for our work and find very good agreement between the MFT and MCS results, which lends credence to our MFT.

The precise forms of the phase boundaries that we obtained do depend upon the choices of the specific forms for the functions f and g that we have chosen to work with; see Eq. (2) together with Eqs. (3) and (4). It behooves us to discuss the degree of generality of our results. We notice that in a variant of this model, if the sum $f+g$ is any positive number $k \neq 1$, it can be reduced to our model by appropriately rescaling f and g, together with α and β. Thus, the structure of the phase diagrams will remain unchanged when considered in terms of rescaled α and β. One could additionally conceive other more drastic variants of the model, where (2) is replaced by nonlinear relations between f and g, while maintaining the general properties of f and g of being increasing and decreasing functions of the instantaneous reservoir population. While the mathematical forms of the phase boundaries would change, depending upon the precise nonlinear analog of (2), we expect the general qualitative features of the results from our model should continue to hold. For instance, all four phases of our model should be present in some regions of the phase space. We also expect to have only LD or SP phases for very low μ, whereas for very high μ, no delocalization of domain walls is expected. The MFT that we have developed here can be straightforwardly extended to study the effects of various nonlinear variants of (2). Our model may be generalized by changing the precise dependence of α_e and β_e on the reservoir occupation; one could study the sensitivity of

the phase diagram on these dependences. Again, we expect the general conclusions drawn here to hold qualitatively, so long as the monotonic dependences of f and g on N are maintained. It would also be interesting to study the effects of using a different value for the scale N^*. We have used a simple mean-field description to build the broad physical picture of the properties of this model. Applications of more sophisticated analytical methods, e.g., matrix product ansatz [24] or Bethe ansatz [25], successfully applied elsewhere, should be considered in the future.

It would be interesting to introduce diffusive exchanges or Langmuir kinetics between the reservoir and the bulk of the TASEP that do not violate the global conservation of particles, but break it locally in the bulk of the TASEP, and see whether the phase diagram can be changed significantly or new phases can emerge. We have assumed the reservoir to be a point, devoid of any spatial extent and internal dynamics. While this makes the ensuing calculations simple and analytically tractable, this makes it an idealization of more complex situations where internal reservoir dynamics is generically expected. This may be incorporated by using and suitably modifying some of the models studied in Ref. [14]. In addition, multiple TASEP lanes and multiple species of particles along with reactions between them would be an interesting future study that couples driven reactions with overall particle number conservation and crowding effects.

ACKNOWLEDGMENT

A.B. thanks A. K. Gupta for critical comments on the manuscript, and the SERB, DST (India) for partial financial support through the MATRICS scheme (file no. MTR/2020/000406).

[1] C. T. MacDonald, J. Gibbs, and A. Pipkin, Biopolymers **6**, 1 (1968); C. T. MacDonald and J. H. Gibbs, *ibid.* **7**, 707 (1969).

[2] J. Krug, Phys. Rev. Lett. **67**, 1882 (1991); B. Derrida, E. Domany, and D. Mukamel, J. Stat. Phys. **69**, 667 (1992); B. Derrida, S. A. Janowsky, J. L. Lebowitz, and E. R. Speer, *ibid.* **78**, 813 (1993); B. Derrida and M. R. Evans, J. Phys. I France **3**, 311 (1993).

[3] S. A. Janowsky and J. L. Lebowitz, Phys. Rev. A **45**, 618 (1992).

[4] D. A. Adams, B. Schmittmann, and R. K. P. Zia, J. Stat. Mech. (2008) P06009.

[5] L. J. Cook and R. K. P. Zia, J. Stat. Mech. (2009) P02012.

[6] L. J. Cook, R. K. P. Zia, and B. Schmittmann, Phys. Rev. E **80**, 031142 (2009).

[7] P. Greulich, L. Ciandrini, R. J. Allen, and M. C. Romano, Phys. Rev. E **85**, 011142 (2012).

[8] C. A. Brackley, L. Ciandrini, and M. C. Romano, J. Stat. Mech. (2012) P03002.

[9] M. Ha and M. den Nijs, Phys. Rev. E **66**, 036118 (2002).

[10] C. A. Brackley, M. C. Romano, C. Grebogi, and M. Thiel, Phys. Rev. Lett. **105**, 078102 (2010).

[11] C. A. Brackley, M. C. Romano, and M. Thiel, Phys. Rev. E **82**, 051920 (2010).

[12] C. A. Brackley, M. C. Romano, and M. Thiel, PLoS Comput. Biol. **7**, e1002203 (2011); L. Ciandrini, I. Neri, J. C. Walter, O. Dauloudet, and A. Parmeggiani, Phys. Biol. **11**, 056006 (2014).

[13] M. C. Good, M. D. Vahey, A. Skandarajah, D. A. Fletcher, and R. Heald, Science **342**, 856 (2013); J. Hazel, K. Krutkramelis, P. Mooney, M. Tomschik, K. Gerow, J. Oakey, and J. C. Gatlin, *ibid.* **342**, 853 (2013).

[14] P. Roy, A. K. Chandra, and A. Basu, Phys. Rev. E **102**, 012105 (2020).

[15] In detail: MFT is applied on the continuum equation corresponding to the microscopic model, where after neglecting the spatial correlations and taking the continuum limit, one makes the Taylor's expansion $\rho(x+1/L) = \rho(x) + \partial_x\rho(x)/L + (1/2L^2)\partial_x^2\rho(x) + \cdots$, giving particle current $j(x) = \rho(x)[1-\rho(x)]$ neglecting $O(1/L^2)$ contributions in the thermodynamic limit. This suffices in the calculations for the bulk density in the TASEP lane. These terms higher order in $1/L$ should be important in the analysis of the boundary layers of thickness $1/L$ near the edges of the TASEP lane, which is outside the scope of the present work.

[16] In equilibrium systems, where the number density is neither conserved nor critical, the correlations of the number fluctuations are small. In the present problem, neither is the particle number in T conserved (due to the coupling with the reservoir), nor is it a critical variable. Hence, the correlation effects are expected to be small. In out-of-equilibrium systems, however, such wisdom obtained from equilibrium systems may not hold. In the absence of any general result, we can only speculate on the applications of MFT and treat it as a guideline, which is corroborated by our MCS studies. More rigorous approaches on the quantitative accuracy of MFT in the present problem should be welcome.

[17] A. B. Kolomeisky, G. M. Schütz, E. B. Kolomeisky, and J. P. Straley, J. Phys. A: Math. Gen. **31**, 6911 (1998).

[18] H. Hinsch and E. Frey, Phys. Rev. Lett. **97**, 095701 (2006).

[19] T. Reichenbach, T. Franosch, and E. Frey, Phys. Rev. Lett. **97**, 050603 (2006).

[20] N. Sarkar and A. Basu, Phys. Rev. E **90**, 022109 (2014).

[21] T. Banerjee, N. Sarkar, and A. Basu, J. Stat. Mech. (2015) P01024.

[22] T. Banerjee and A. Basu, Phys. Rev. Research **2**, 013025 (2020).

[23] That the domain wall Δ is independent of μ may also be understood heuristically as follows. In the SP phase, as μ changes keeping α and β unchanged, the excess or deficit particles may be accommodated by changing either (i) the reservoir occupation N, (ii) the domain wall height Δ, (iii) the domain wall position x_w, or all or some of them together. Possibilities (i) and (ii) would have to happen together, if at all, since α_e, β_e (which control the height) are related to the reservoir occupation. Hence, a change in N would then automatically imply changes in α_e [through Eq. (7)] and β_e [through Eq. (8)]. Therefore, if these two possibilities were to be adopted by the system, and if there was a domain wall at some (α, β), there would not be any domain wall now when μ is changed to μ', as $\alpha_e(\mu') \neq \beta_e(\mu')$ now. Thus a domain wall could exist for a given (α, β) only for a particular value of μ; a small

change in μ to μ' would result in the system moving to the LD [if $\alpha_e(\mu') < \beta_e(\mu')$] or HD [if $\alpha_e(\mu') > \beta_e(\mu')$] phases completely. This necessarily leads to a rise in the steady state current. On the other hand, with possibility (iii) all the excess or deficit particles are accommodated by shifting the domain wall position x_w keeping the height Δ intact (and also keeping the reservoir occupation N intact). This ensures that the current is unchanged, independent of μ within the SP phase. Thus, within a minimum steady state current principle, possibility (iii) is the acceptable solution.

[24] B. Derrida, M. R. Evans, V. Hakim, and V. Pasquier, J. Phys. A: Math. Gen. **26**, 1493 (1993).

[25] S. Prolhac and K. Mallick, J. Phys. A: Math. Theor. **41**, 175002 (2008).